

# NUMERICAL STUDY AND EVALUATION OF THE SHEAR CAPACITY OF SCREW DOUBLE-SHEAR CONNECTIONS

Wen-Hao Liu<sup>1,2</sup>, Lu Deng<sup>2,3</sup>, Yu-Long He<sup>2,\*</sup>, Tao Wang<sup>1,2</sup> and Huan Liu<sup>2</sup>

<sup>1</sup>Key Laboratory of Concrete and Prestressed Concrete Structures of Ministry of Education, Southeast University, Nanjing 210096, China

<sup>2</sup>College of Civil Engineering, Hunan University, Changsha 410082, Hunan, China

<sup>3</sup>Key Laboratory for Damage Diagnosis for Engineering Structures of Hunan Province, Hunan University, Changsha 410082, Hunan, China

\* (Corresponding author: E-mail: heyl@hnu.edu.cn)

## ABSTRACT

Previous studies have primarily focused on the performance of screw single-shear connections (SSCs) and rarely investigated the performance and calculation methods of screw double-shear connections (DSCs). The first study examines the effect of various parameters on the shear capacity of single-screw DSCs. The results indicate that the steel strength, steel plate thickness, screw diameter, and connection method have significant effects on the shear capacity of thin steel screw DSCs. Specifically, when the steel strength increases from 235 MPa to 550 MPa, the maximum increase in the shear capacity is 81.2%. An increase in steel plate thickness from 0.8 mm to 3.0 mm results in a minimum increase of 34.6% in shear capacity. Similarly, increasing the screw diameter from 3.5 mm to 6.3 mm leads to at least a 35.2% increase in shear capacity. Moreover, changing from the SSC to DSC can result in a maximum increase of 95.4% in shear capacity. Next, the shear performance of screw group DSCs is analyzed parametrically. It is found that when the steel plate thickness is 3.0 mm and the number of screws increases to 3, the failure mode transitions from a coupled bearing and shear failure to bearing failure. Additionally, when the number of screws increases from 2 to 5, the shear capacity of screw group DSCs increases by at least 9.6%. The effect of screw spacing on shear capacity decreases as the number of screws increases, while variations in screw arrangement have minimal impact on shear capacity. Furthermore, increasing the steel plate thickness from 0.8 mm to 1.2 mm results in a minimum 51.1% increase in shear capacity, and increasing the thickness from 1.2 mm to 3.0 mm leads to at least an 88.0% increase in shear capacity. Finally, the results of the parametric analyses are used to evaluate the applicability of design equations for screw DSCs. The findings indicate that the AISC specification provides accurate predictions for single screw DSCs, regardless of whether bearing or shear failure occurs. In contrast, for screw group DSCs, the AISC predictions tend to be conservative when the specimen experiences coupled bearing and shear failure, and unsafe when bearing failure occurs.

Copyright © 2025 by The Hong Kong Institute of Steel Construction. All rights reserved.

## ARTICLE HISTORY

Received: 18 March 2024  
Revised: 6 January 2025  
Accepted: 8 January 2025

## KEYWORDS

Double-shear connections (DSCs);  
Screw group connection;  
Shear capacity;  
Failure modes;  
Design formula

## 1. Introduction

Cold-formed steel (CFS) structures are widely used in low-rise buildings around the world [1]. However, key challenges in the development of mid- and high-rise CFS buildings include the low shear capacity and inadequate lateral stiffness of combined shear walls [2]. The lateral resistance of these walls is directly influenced by the diaphragm effect of the sheathings, and reliable screw connections between the sheathings and light-gauge steel studs are crucial to ensuring the diaphragm effect functions properly, thereby guaranteeing the structural load-carrying capacity [1]. As a critical shear connection element, the shear performance of screw connections significantly impacts the load-carrying capacity of the entire connected system. Therefore, examining the shear performance of screw connections is essential.

Considerable efforts and contributions have been made by numerous scholars in investigating the shear performance of screw connections. Pekoz [3] summarized the results of over 3500 tests on screw connections and developed design provisions. Rogers et al. [4] found that the predicted values from AS/NZS4600, CSA-S136, and AISI codes were unsafe when fastening two steel plates with different thicknesses. Laboube and Sokol [5-7] revealed a significant “screw group effect” in screw connections. Experimental research by Roy et al. [8] and Huynh et al. [9] demonstrated that screw arrangement affects the strength of the connection. Moreover, Huynh et al. [10] proposed a modified design formula for screw connections. Vy et al. [11] concluded that the tilting and bearing capacity design methodologies for screw connections in current standards are reliable at ambient temperatures. For elevated temperature, the shear capacity must be multiplied by a reduction factor accounting for the temperature effect. Lu et al. [12] presented modified equations for determining the shear capacity of screw connections at both ambient and elevated temperatures. Chen et al. [13] experimentally examined the single-shear behavior of screw connections between CFSs at different temperatures and explored the influence of screw diameter, steel type, and plate thickness on shear capacity. Guan et al. [14] developed a detailed FE model to investigate the effect of various parameters on the shear behavior of screw connections. Chen et al. [15] conducted experimental studies on the shear capacity and failure modes of screw connections between steel-timber composite structures. Feng et al. [16] concluded that the screw diameter and plate thickness greatly affect the shear capacity of screw connections. Lu et al. [17] identified limitations in the design equations of existing codes for predicting the shear capacity of screw groups.

Through literature research, the authors have found that screw DSCs are

primarily used in midply shear wall (MSW) structures [2, 18-25], as illustrated in Fig. 1. In MSWs, the sheathing is placed in the center of the wall, sandwiched between the two side studs and the upper and lower tracks. Notably, the studs in MSWs are rotated by 90° relative to those in traditional shear walls, with screws passing through the studs, sheathing, and studs in sequence. This change results in a shift from single-shear to double-shear force mechanisms, significantly enhancing the shear capacity and lateral stiffness of MSWs [18-21]. Experimental studies by Varoglu et al. [18-19] revealed that the shear capacity and lateral stiffness of wood MSW are 2 to 3 times greater than those of traditional wood shear walls. Zhou et al. [22] and Brière et al. [23] investigated the seismic performance of CFS-MSWs and concluded that their shear capacity and lateral stiffness are 2 to 4 times higher than those of traditional CFS shear walls. Based on the theoretical design equations proposed by Yanagi et al. [26] for determining the shear capacity of steel plate shear walls, it can be concluded that using design equations for screw SSCs to estimate the shear capacity of MSWs is conservative.

However, existing studies have predominantly focused on the shear performance of screw SSCs, with limited attention given to screw DSCs. Zhou et al. [27] conducted monotonic and cyclic loading tests on the shear performance of nail SSCs and DSCs, demonstrating that the shear capacity and stiffness of nail DSCs are significantly higher than those of nail SSCs. Liu [28] performed an experimental study on single-screw DSCs for thicker steel plates and derived corresponding design equations. However, the influence of various parameters on the shear capacity of single-screw DSCs remains unclear. Despite the aforementioned research efforts, there is a lack of studies addressing the shear performance of screw group DSCs, and the existing shear capacity design equations are applicable only to screw SSCs. Further verification is required to assess whether these equations are suitable for predicting the shear resistance of screw DSCs.

Based on the problems mentioned above, this study aims to adopt the verified FE model to investigate the shear performance of both single screw and screw group DSCs. The study explores the influence of various parameters, including sheet strength and thickness, screw diameter, screw connection type, number of screws, screw spacing, and screw arrangement, on the failure modes and shear capacity of single screw and screw group DSCs. Finally, the results of the parametric analyses are used to evaluate the applicability and feasibility of the design formulas for single screw or screw group DSCs, as proposed by AISI S100-2016 [29], GB 50018-2002 [30], EN 1993-1-3:2006 [31], and AISC 360-16 [32].

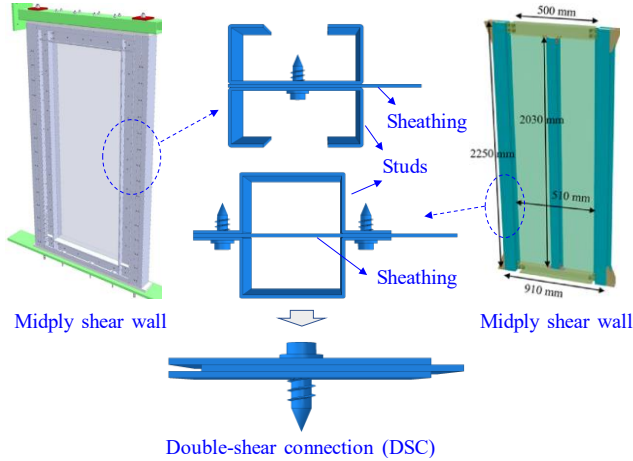


Fig. 1 Application of screw DSCs

## 2. Modeling and validation

### 2.1. FE model

The FE models of screw DSC and SSC were established based on the test specimen geometry in the literature [28]. The dimensions of the steel plate were  $220 \text{ mm} \times 50 \text{ mm}$ , with sheet thickness ( $T$ ) ranging from 3.0 mm to 6.0 mm. The steel plate was made of Q235 steel, and the mechanical properties were obtained from tensile coupon tests [28]. It is noted that the overlap length between steel plates was 60 mm, and three different screw diameters ( $D$ ) were used: 4.8 mm, 5.5 mm, and 6.3 mm. To prevent tearing failure at the ends and edges of the plates, the screw end and edge distances were 30 mm and 25 mm, respectively. Notably, the distance from the center of the screw hole to the end of the plate satisfies the general code requirement of being greater than  $3D$ .

The FE model of screw DSC and SSC is shown in Fig. 2. Due to the complex structure of the screw, modeling and meshing become challenging. Additionally, the intricate contact between the threads and the steel plate may cause convergence issues in the calculation, leading to significantly higher computational costs. To address these challenges, simplifications were made to the screw solid model, based on the screw modeling methods outlined in the

literature [8,33]. The simplifications include: (1) treating the screw and washer as a single solid unit; (2) simplifying the screw head and threaded shank into a cylinder shape; (3) neglecting any damage to the steel plate or the screw during the drilling process; and (4) disregarding the preload force generated in the steel plate by the screw.

Comment 3: The manuscript mentions several simplifications in the FE model (e.g., ignoring the preload force, thread interactions, and damage to the steel plates during drilling). While these are justified for computational efficiency, the potential impact of these assumptions on the accuracy of results should be discussed more explicitly.

During modeling, C3D8R elements are used for all model components. The steel constitutive model adopts an ideal elastic-plastic model, considering material hardening effects. The elastic modulus ( $E$ ) was set at 206 GPa, the second modulus was  $0.01E$ , and Poisson's ratio ( $\nu$ ) was 0.3. Since self-drilling screws are primarily made of carbon steel, which exhibits brittle fracture when the ultimate strength is reached, the ductile damage criterion is adopted for the screws. The fracture strain and stress triaxiality values were referenced from the literature [8, 34]. After repeated trial calculations and calibration, the fracture strain and stress triaxiality values in this study were 0.762 and 0.207, respectively. Moreover, the elastic modulus and ultimate strength of the screws were 206 GPa and 1250 MPa, respectively [1]. Considering the stress concentration caused by the screw threads, the stress concentration factor was set at 1.79 [35], and the effective ultimate strength was taken as 700 MPa. Contact pairs are defined between steel plates and between steel plates and self-drilling screws. The contact properties include hard contact in the normal direction and tangential behavior governed by the penalty method, with a friction coefficient of 0.3. In the screw DSC model (see Fig. 2(a)), the right ends of the upper and lower steel plates are fully fixed, and a displacement load was applied in the U1 direction at the coupling point RP-1 on the left end of the middle plate. The boundary constraints and applied loads for the screw SSC model (see Fig. 2(b)) are identical to those for the screw DSC model. The maximum displacement, based on the load-displacement curves derived from the tests, was applied to the FE model. For consistency, the displacement load at RP-1 is set to 6 mm. It should be noted that the mesh was refined at the locations where the stresses are concentrated, and coarser mesh elements were used in areas of lower stress. To capture the stress concentration area effectively, the area had a side length of 30 mm, as shown in Fig. 2. To avoid convergence issues due to complex interactions between the screws and the holes in the steel plate, an explicit dynamic solver was employed.

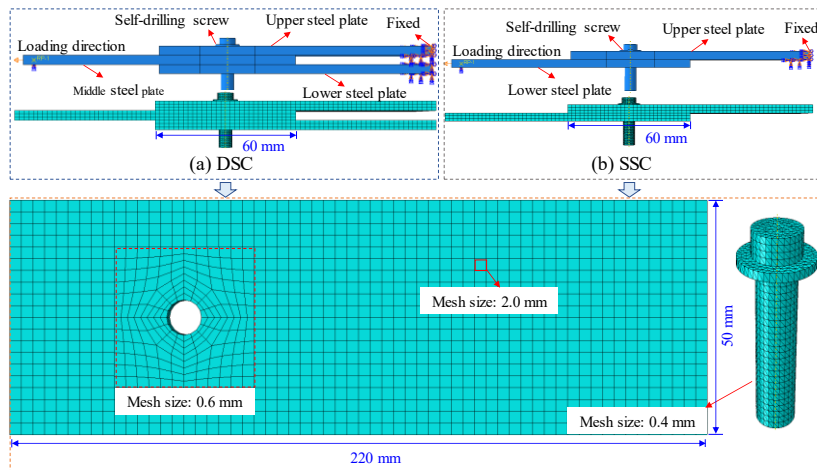


Fig. 2 FE model

### 2.2. Model validation

To further validate the accuracy of the established FE model, the numerical results were compared with the experimental results.

#### 2.2.1. Failure modes

Experimental studies [28] have shown that the failure modes of single screw DSCs can be classified into three types: bearing failure, coupled bearing and shear failure, and shear failure. When bearing failure occurred in screw DSCs (see Fig. 3(a)), the middle steel plate near the screw hole experienced significant plastic deformation along the thickness direction, while the screw shank produced notable bending without shearing. This failure mode exhibits clear warning signs before the specimen fails, indicating ductile damage. When coupled bearing and shear failure occurred in screw DSCs, self-drilling screw shear fracture was accompanied by noticeable deformation near the hole wall of

the middle steel plate, the shear failure surface formed at the junction of the steel plates, as depicted in Fig. 3(b). When shear failure occurred in screw DSCs, the screw shank developed two shear failure surfaces, and these failure surfaces are smooth. The failure surfaces occurred in the junction of the steel plates. In addition, as demonstrated in Fig. 3(c), when shear failure occurred, the screw head remained perpendicular to the steel plate, while the screw bottom tilted slightly. There is no significant deformation of the screw holes, and no clear warning signs precede the failure, indicating a brittle failure.

In addition, experimental studies have shown that the failure modes of single-screw SSCs can be classified into two types: shear failure and screw tilting accompanied by steel plate warping, as illustrated in Fig. 4. It is found that there is no noticeable deformation near the screw hole before screw shear failure, and no warning signs are evident, indicating brittle failure. When screw tilting and steel plate warping occurred, the screw shank produced significant plastic deformation, with the screw shank tilting in the direction of the applied

force.

Compared to the failure modes of screw SSCs, screw DSCs exhibit a key difference: during bearing failure, the middle steel plate near the screw holes undergoes significant plastic deformation along the thickness direction. As shown in the stress distribution diagram, the screw-bearing region in DSCs is approximately rectangular, whereas the screw-bearing region in SSCs is

triangular. For screw DSCs, the specimen typically experiences coupled bearing and shear failure, the phenomenon not observed in single-screw SSCs. In the case of shear failure, DSCs have two smooth shear failure surfaces, while SSCs only have one.

Comparing the failure modes concluded from the tests and simulations, it is found that the failure modes of the two are in good agreement.

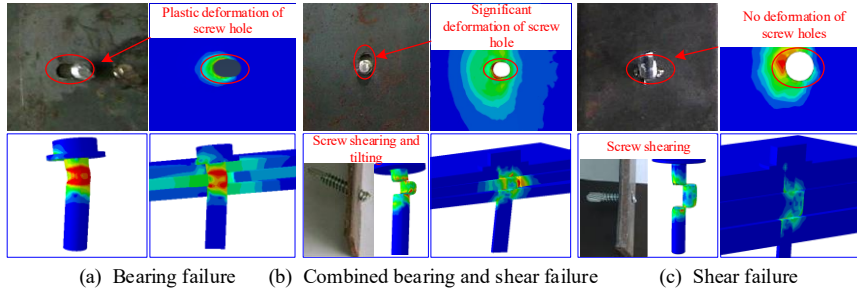


Fig. 3 Failure modes validation for DSCs

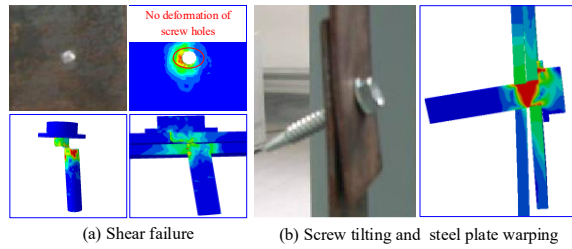


Fig. 4 Failure modes validation for SSCs

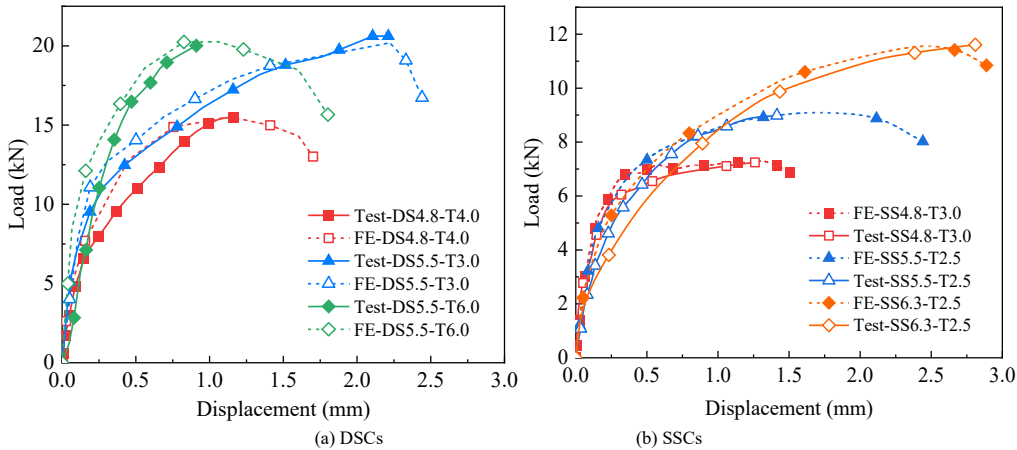


Fig. 5 Comparison of load versus displacement curves

2.2.2. Load versus displacement curves

Fig. 5 compares the load versus displacement curves obtained from tests and simulations. It can be observed that the load-displacement curves for screw DSCs or SSCs can be classified into three phases. Initially, during the loading phase, the screw connections behave elastically. As loading continues, the stiffness of screw connections gradually decreases, plastic deformation increases, and the load grows nonlinearly with the displacement, which corresponds to the plastic phase. Finally, when the shear capacity of screw DSCs reaches its peak value, displacement and deformation continue to increase, but the shear capacity suddenly decreases, and the stiffness becomes negative, signaling the failure stage. These findings are generally consistent with the analyses presented in the literature [28]. Due to the inevitable damage during specimen fabrication, the simulation results tend to be higher than the test results. Overall, the load-displacement curves for both screw DSCs and SSCs are well simulated using the FE method.

2.2.3. Shear capacity

Fig. 6 compares the shear capacity of single screw DSCs and SSCs obtained from both tests and simulations. It is seen that the test and FE values for both screw DSCs and SSCs are in good agreement. Statistical analysis indicates that the average value of  $P_{Test}/P_{FE}$  of screw DSCs is 1.01, with a coefficient of variation of 2.67%, and the absolute value of the error does not exceed 5%. The average value of  $P_{Test}/P_{FE}$  of screw SSCs is 1.00, with a coefficient of variation of 0.93%, and an absolute value of error does not exceed 2%. These results demonstrate that the FE model can simulate the shear capacity of screw DSCs

and SSCs with high accuracy.

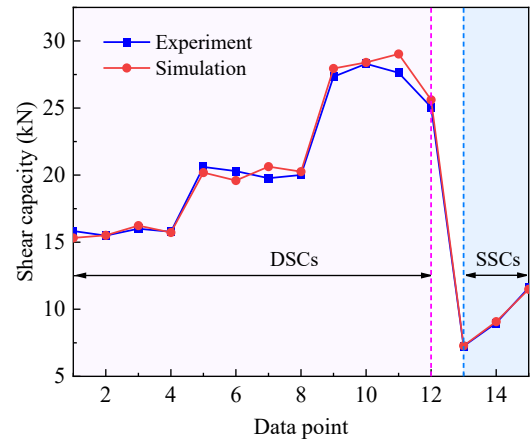


Fig. 6 Comparison of test values with FE values

2.2.4. Summary

Based on the analysis in subsections 2.2.1 to 2.2.3, the results demonstrate that the FE model accurately replicates the shear performance of screw DSCs and SSCs, making it suitable for subsequent parametric studies.

### 3. Shear capacity analysis for single screw DSCs

This section discusses the influences of steel strength, sheet thickness, screw diameter, and screw connection types on the shear capacity of specimens, based on validated FE models. The steel strengths considered are Q235, Q345, Q460, and Q550, with corresponding material properties provided in Table 1. Four different sheet thicknesses are used: 0.8 mm, 1.2 mm, 3.0 mm, and 6.0 mm. The screw diameters considered are 3.5 mm, 4.8 mm, 5.5 mm, and 6.3 mm. The screw connection types include single-shear and double-shear configurations.

**Table 1**  
Material properties of steel [36-37]

Steel strength	$f_y$ (MPa)	$f_u$ (MPa)	$E$ (GPa)	$\epsilon_y$	$\epsilon_u$
Q235	235	305	206	0.0011	0.0351
Q345	345	448	206	0.0017	0.0517
Q460	460	550	206	0.0022	0.0459
Q550	550	670	206	0.0027	0.0609

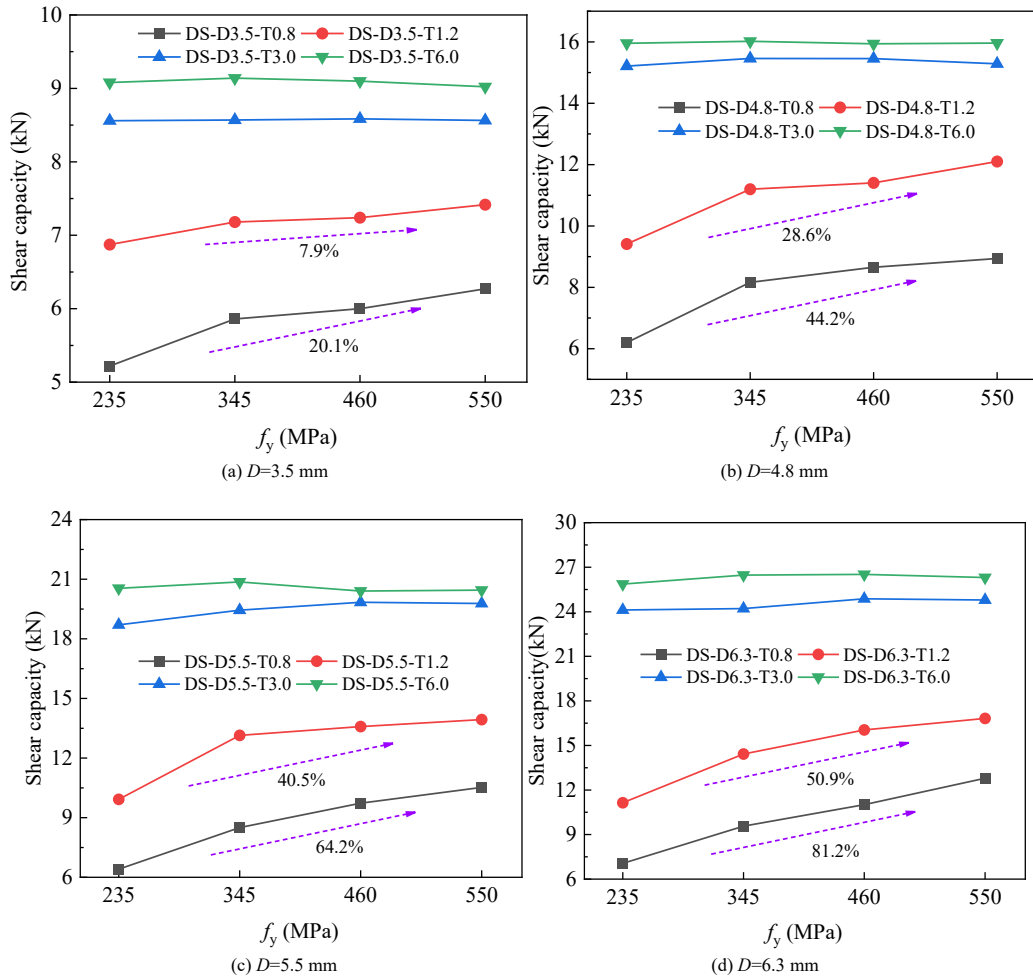


**Fig. 7** The influence of steel strength

#### 3.2. The influence of sheet thickness

Fig. 8 gives the relationship curves of the shear capacity of single screw DSC specimens with sheet thicknesses ( $T$ ). It is found that the shear capacity rises with the increase of  $T$  and eventually stays almost unchanged. Specifically, the shear capacity of screw DSCs increases by at least 34.6% and up to 241.8% as  $T$  grows from 0.8 mm to 3.0 mm. This increase is attributed to the larger bearing area provided by the thicker plate, which significantly enhances the shear capacity. However, as  $T$  exceeds 3.0 mm, the influence of further increases in  $T$  on shear capacity becomes negligible. This is because, beyond this threshold, shear failure becomes the dominant failure mode, and the shear capacity is controlled by the screw strength. Specifically, when  $T$  increases from 3.0 mm to 6.0 mm, the maximum increment in shear capacity is only 9.8%.

#### 3.1. The influence of steel strength

The relationship curves of the shear resistance of screw DSCs with the change of steel strength are plotted in Fig. 7. It is observed that for  $T$  not exceeding 3.0 mm, the shear capacity of screw DSCs increases with steel strength. This is primarily due to bearing failure being the dominant mode of failure for smaller values of  $T$ , where the shear capacity is mainly controlled by the plate strength. A minimum of 7.9% increase in shear capacity is achieved when the steel strength is increased from 235 MPa to 550 MPa. In addition, as  $D$  increases, the influence of steel strength on the shear resistance becomes more pronounced. The maximum increase in shear capacity from 235 MPa to 550 MPa was 81.2% when  $D$  was increased to 6.3 mm. However, when  $T$  exceeds 3.0 mm, shear failure becomes more prevalent, and the shear capacity is primarily determined by the screw strength. In this case, the effect of steel strength on the shear capacity of single screw DSCs is minimal, with a change in shear capacity of less than 5%.

#### 3.3. The influence of screw diameter

The relationship curves between shear capacity and screw diameter ( $D$ ) are presented in Fig. 9. It is seen that the shear capacity of screw DSCs rises almost linearly with an increase in  $D$ . From Fig. 9(a)-(b), it is noticed that when  $D$  increases from 3.5 mm to 6.3 mm, the shear capacity increases by at least 35.2% and 62.2%, respectively. This is due to the increased bearing area resulting from the larger screw diameter, which in turn enhances the shear capacity. The influence of increasing  $D$  on shear capacity is more pronounced as the steel strength increases, as the shear capacity under bearing failure is positively correlated with both the steel strength and bearing area. As shown in Fig. 9(c)-(d), when  $T$  exceeds 3.0 mm, the shear capacity curves of different steel strengths almost overlap, indicating that the influence of increasing  $D$  on shear capacity becomes similar across different steel strengths. This is mainly because, for  $T$  exceeding 3.0 mm, the screw shank is exposed to shear failure.

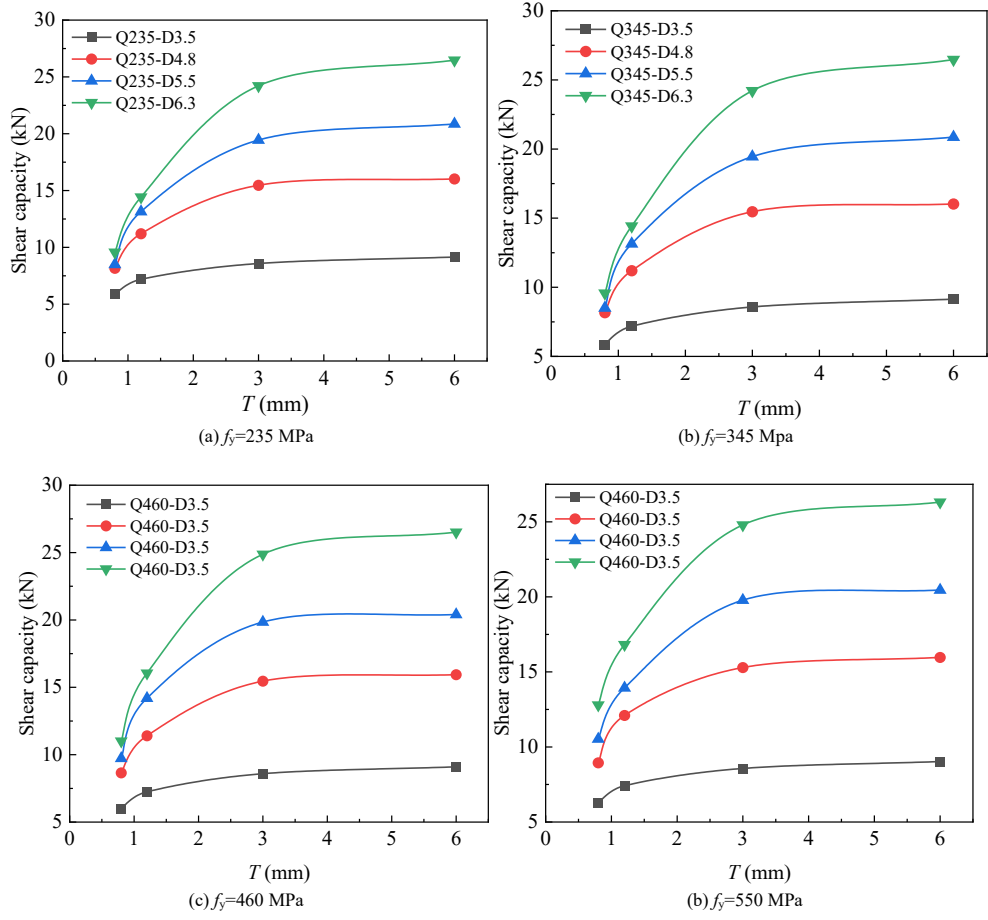


Fig. 8 The effect of  $T$

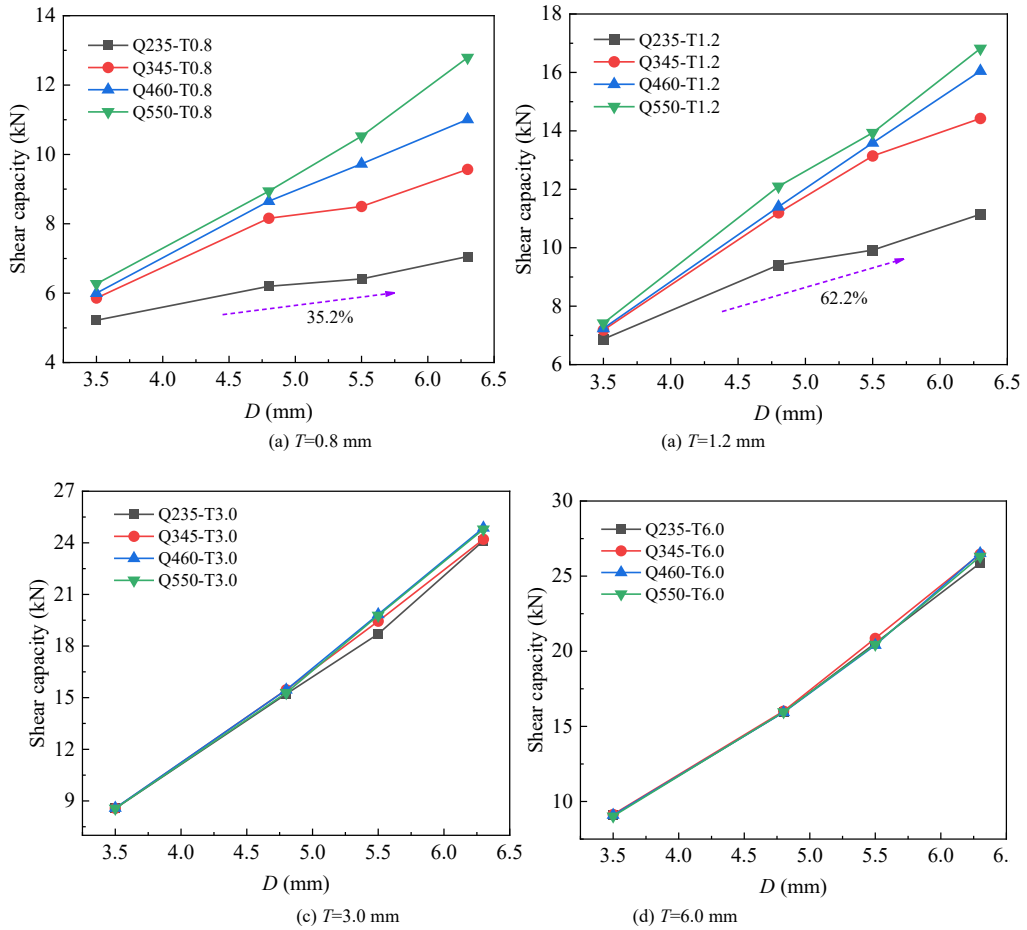


Fig. 9 The effect of  $D$

3.4. The influence of screw connection type

To investigate the influence of screw connection type on the shear behavior, 54 specimens were prepared for comparative analysis in this subsection. The steel strengths used were Q235, Q345, and Q420, the sheet thicknesses were 0.8 mm, 1.2 mm, and 2.0 mm, and the screw diameters included three types: 4.8 mm, 5.5 mm, and 6.3 mm. The screw connection types considered were single-shear and double-shear configurations. Figs. 10-12 illustrate the impact of different screw connection types on shear capacity for various parameters. These figures show that the shear capacities of single-screw DSCs are significantly higher than those of single-screw SSCs. In addition, Table 2 lists the FE values of shear

capacity for 54 sets of specimens. It is observed that when the screw connection type changes from single-shear to double-shear, the shear capacity increases by at least 30.9%, with a maximum increase of 95.4%. During bearing failure, the middle steel plate of DSCs is constrained by the upper and lower steel plates, allowing for a more efficient utilization of the steel strength. In the case of shear failure, DSCs have two shear surfaces, while SSCs only have one, resulting in a significantly higher shear capacity for DSCs compared to SSCs. Notably, the screw connection type also changes the failure mode of specimens. Specifically, when  $T$  increases to 2.0 mm, screw SSCs experience coupled bearing and shear failure, while screw DSCs mainly undergo bearing failure.

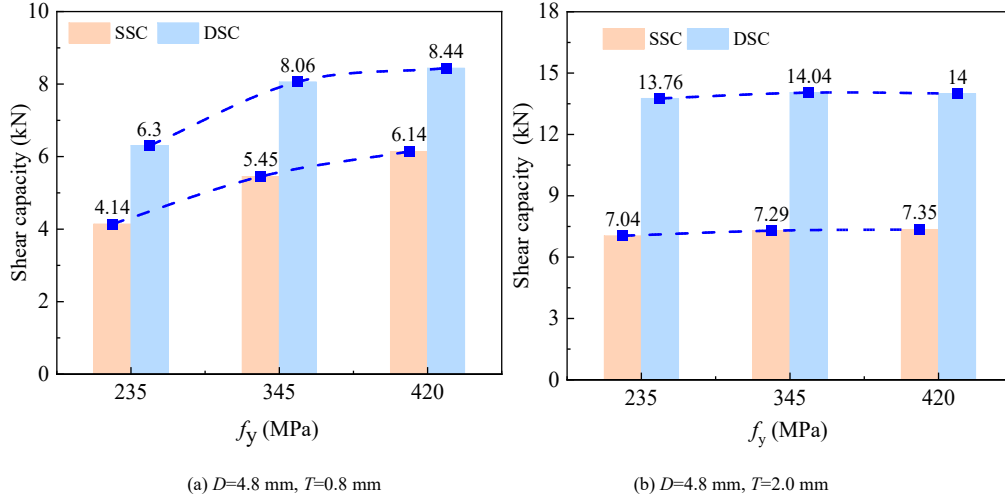


Fig. 10 The influence of steel strength

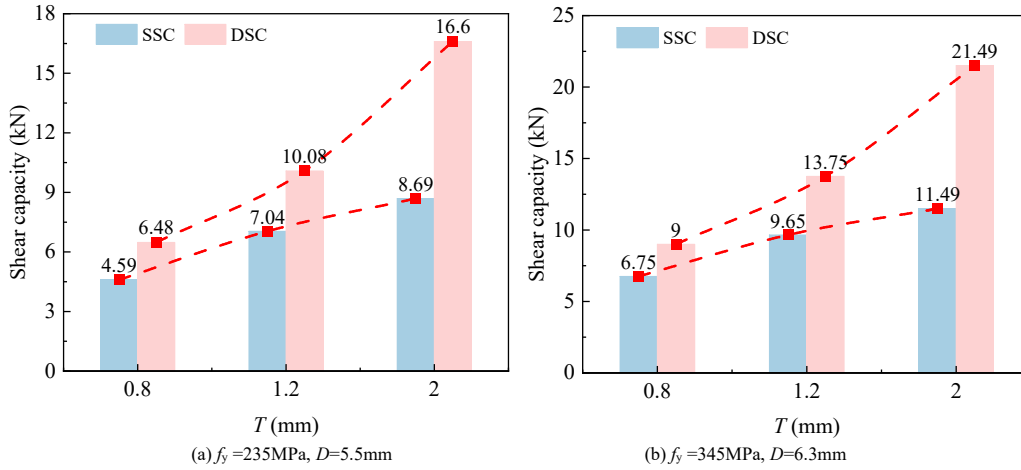


Fig. 11 The influence of  $T$

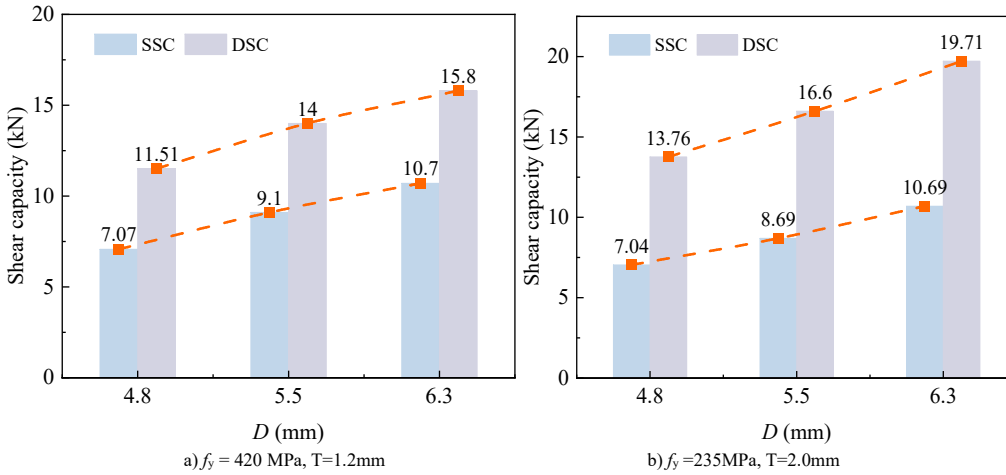


Fig. 12 The influence of  $D$

**Table 2**  
The effect of screw connection type on shear capacity and failure modes

No.	Specimen name	$P_u$ (kN)		Failure mode		$\frac{P_{u-DSC} - P_{u-SSC}}{P_{u-SSC}} \times 100\%$
		DSC	SSC	DSC	SSC	
1	Q235-D4.8-T0.8	6.30	4.14	B	B	52.2%
2	Q235-D4.8-T1.2	9.39	6.13	B	B	53.2
3	Q235-D4.8-T2.0	13.76	7.04	B	B+S	95.5%
4	Q235-D5.5-T0.8	6.48	4.59	B	B	41.2%
5	Q235-D5.5-T1.2	10.08	7.04	B	B	43.2%
6	Q235-D5.5-T2.0	16.60	8.69	B	B+S	91.0%
7	Q235-D6.3-T0.8	6.65	5.08	B	B	30.9%
8	Q235-D6.3-T1.2	10.68	7.38	B	B	44.8%
9	Q235-D6.3-T2.0	19.71	10.69	B	B+S	84.4%
10	Q345-D4.8-T0.8	8.06	5.45	B	B	48.0%
11	Q345-D4.8-T1.2	11.32	7.02	B	B	61.3%
12	Q345-D4.8-T2.0	14.04	7.29	B	B+S	92.4%
13	Q345-D5.5-T0.8	8.68	6.06	B	B	43.3%
14	Q345-D5.5-T1.2	13.17	8.66	B	B	52.1%
15	Q345-D5.5-T2.0	17.34	9.17	B	B+S	89.1%
16	Q345-D6.3-T0.8	9.00	6.75	B	B	33.4%
17	Q345-D6.3-T1.2	13.75	9.64	B	B	42.6%
18	Q345-D6.3-T2.0	21.49	11.49	B	B+S	87.1%
19	Q420-D4.8-T0.8	8.44	6.14	B	B	37.6%
20	Q420-D4.8-T1.2	11.51	7.07	B	B	62.9%
21	Q420-D4.8-T2.0	14.00	7.35	B	B+S	90.4%
22	Q420-D5.5-T0.8	9.64	6.83	B	B	41.3%
23	Q420-D5.5-T1.2	14.00	9.10	B	B	53.8%
24	Q420-D5.5-T1.2	17.53	9.30	B	B+S	88.4%
25	Q420-D6.3-T0.8	10.39	7.70	B	B	35.0%
26	Q420-D6.3-T1.2	15.80	10.70	B	B	47.7%
27	Q420-D6.3-T2.0	21.56	11.67	B	B+S	84.7%

Notes: “B” represents bearing failure; “S” denotes shear failure.  $P_{u-DSC}$  and  $P_{u-SSC}$  denote the shear capacity of screw DSCs and SSCs, respectively.

**4. Shear capacity analysis for screw group connections**

Although Section 3 provided a parametric analysis of the shear capacity of single-screw DSCs, in practical engineering, components are typically connected using two or more screws. Previous research has demonstrated a remarkable group effect on the shear capacity of screw group SSC specimens [5-7]. To gain a deeper understanding of the shear performance of screw group DSCs, this section discusses the effects of various parameters on shear capacity and failure modes.

**4.1. Model parameters**

In this study, four parameters are considered: the number of screws, screw

spacing and arrangement, and steel plate thickness. The number of screws ( $n$ ) is 2, 3, 4, and 5. The screw spacing ( $s$ ) is defined as  $2D$ ,  $3D$ , and  $4D$ , where  $D$  adopts 4.8 mm. The screw arrangement is divided into two types, A and B, as indicated in Fig. 13. The steel plate thicknesses ( $T$ ) are 0.8 mm, 1.2 mm, and 3.0 mm, respectively, with Q235 steel strength. As an example, S2-A-3D-T3.0 indicates a configuration where S2 denotes 2 screws with arrangement A, 3D represents a screw spacing of 3 times the screw diameter, and T3.0 denotes a steel plate thickness of 3.0 mm. It is noted that when  $n$  is increased to 5 and  $s$  is raised to  $4D$ , the screw connection no longer satisfies the specification requirements. Therefore, when  $n$  reaches 5, only  $s$  of  $2D$  and  $3D$  are considered. In total, 42 specimens were prepared to investigate the shear performance of screw group DSCs with different parameters.

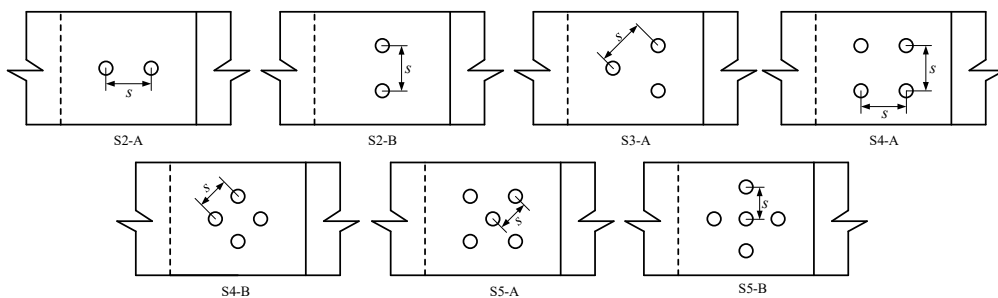


**Fig. 13** Number and arrangement of screws

**4.2. Failure modes**

Based on the FE results, the failure modes of screw group DSCs can be

classified into two categories: bearing failure and coupled bearing and shear failure. Fig. 14 exhibits typical failure modes for 14 specimens. When  $T$  is less than 3.0 mm or  $n$  exceeds 2, the specimen primarily experiences bearing failure.

When  $T$  reaches 3.0 mm and  $n$  is 2, the specimen mainly undergoes coupled bearing and shear failure. As indicated in Fig. 14(a), when  $n = 2$ , the screw arrangement is A, and  $T = 0.8$  mm, the specimen is primarily subjected to bearing failure. In this case, the deformation of screw holes in the middle plate, near the forced end, is larger than that of the screw holes farther from the forced end, and there is no significant deformation of the screw shank. However, when the screw arrangement is changed to B, the deformation of the two screw holes in the middle steel plate remains almost identical, with no noticeable deformation of the screw shank, as illustrated in Fig. 14 (b). When  $T$  increases to 3.0 mm, the specimen undergoes coupled bearing and shear failure, as displayed in Fig. 14 (c)-(d). In this failure mode, the screw holes in the middle steel plate experience significant plastic deformation, the screws exhibit a shear failure surface, and the failure surface occurs at the junction of the upper and the middle steel plates. In addition, a significant shear deformation in the screw shank is observed at the

junction of the lower and the middle steel plates. When  $n$  exceeds 2, the specimens primarily experience bearing failure, as shown in Fig. 14(e)-(n). In this case, the screw holes in the middle steel plate near the forced end undergo obvious plastic deformation, while those farther from the forced end deform less. The screw holes in the upper and lower plates show no visible deformation. As  $T$  increases (see Fig. 14(f), (h), (j), (l), and (n)), the screw shank produces significant bending deformation. However, as  $n$  increases, the bending deformation of the screw shank decreases.

It is concluded that both  $n$  and  $T$  significantly influence the failure mode of screw group DSCs. However, when the number of screws exceeds 2, further increases in the number of screws do not affect the failure mode. Within the specified range of screw spacing, neither the spacing nor the arrangement has a significant impact on the failure mode. However, it is noted that the screw arrangement affects the degree of plastic deformation in the screw holes.

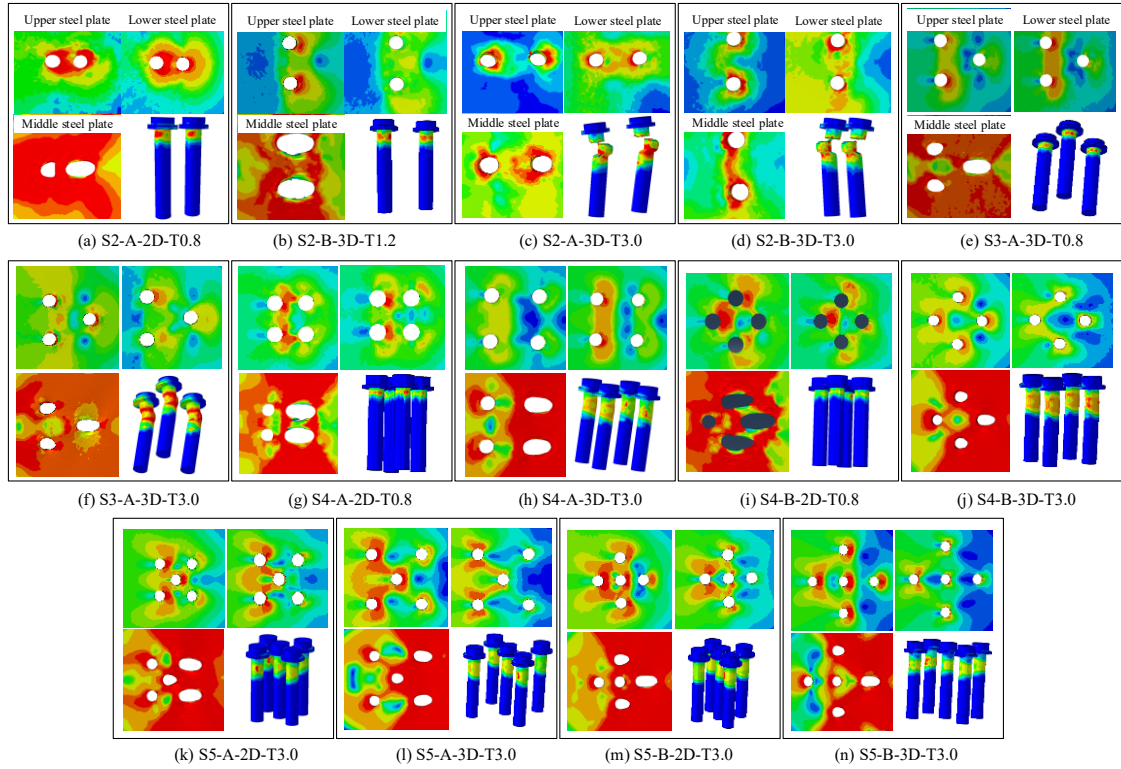


Fig. 14 Failure mode of screw group DSCs

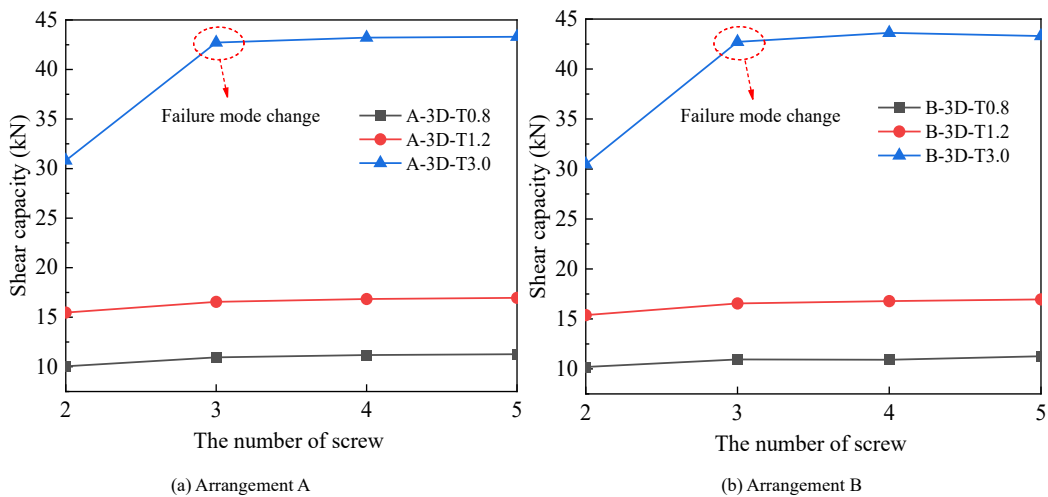


Fig. 15 Effect of  $n$  on shear capacity

### 4.3. Parametric analysis

#### 4.3.1. The influence of the number of screws

Fig. 15 presents the relationship curves for the variation of shear capacity of screw group DSCs with  $n$ . It is observed that the shear capacity increases as  $n$  increases. When  $T$  is 0.8 mm or 1.2 mm, the effect of increasing  $n$  on the shear capacity is minimal. Specifically, when  $n$  increases from 2 to 5, the shear capacity increases by 12.1% and 9.6% for screw arrangement A, and by 10.5%

and 10.2% for screw arrangement B, respectively. This indicates that for smaller values of  $T$ , the specimens primarily experience bearing failure, and the screw strength is not fully utilized, so increasing  $n$  has a limited effect on the shear capacity. However, when  $T$  increases to 3.0 mm and  $n$  rises from 2 to 3, the shear capacity increases by 38.7% and 40.2% for screw arrangements A and B, respectively. When the number of screws increases further from 3 to 5, the shear capacity remains largely unchanged. This suggests that at  $T = 3.0$  mm, specimens connected with 2 screws experience coupled bearing and shear failure, and the shear capacity is mainly governed by the screw strength. However, when

$n$  increases to 3, the failure mode changes from coupled bearing and shear failure to bearing failure, which is mainly controlled by the strength of the steel plate. Therefore, the increase in shear capacity is notably influenced when  $n$  rises from 2 to 3, but further increases in  $n$  (from 3 to 5) have little impact, as the failure mode remains bearing failure.

4.3.2. The influence of screw spacing

Fig. 16 presents the relationship curves showing the variation in the shear capacity of screw group DSC specimens to screw spacing. From Fig. 16(a)-(b), it is observed that when  $n$  is 2 and  $T$  is 0.8 mm or 1.2 mm, the shear capacity of screw group DSCs increases as  $s$  increases. Specifically, when  $s$  increases from

2D to 4D, the shear capacity increases by up to 15.2%, with a minimum increase of 12.1%. When  $T$  is increased to 3.0 mm, the effect of  $s$  on shear capacity becomes negligible, with the maximum change in shear capacity being only 2.0%. From Fig. 16(c)-(d), it is seen that when  $n$  is increased to 4, the effect of  $s$  on shear capacity diminishes, with the maximum amplitude change being only 7.4%. Similarly, from Fig. 16 (e)-(f), when  $n$  is raised to 5 and  $s$  is increased from 2D to 3D, the maximum increase in shear capacity for screw group DSCs with different plate thicknesses is 7.1%, 9.6%, and 1.5%, respectively. Overall, it can be concluded that the effect of screw spacing on the shear capacity of screw group DSCs decreases as the number of screws increases.

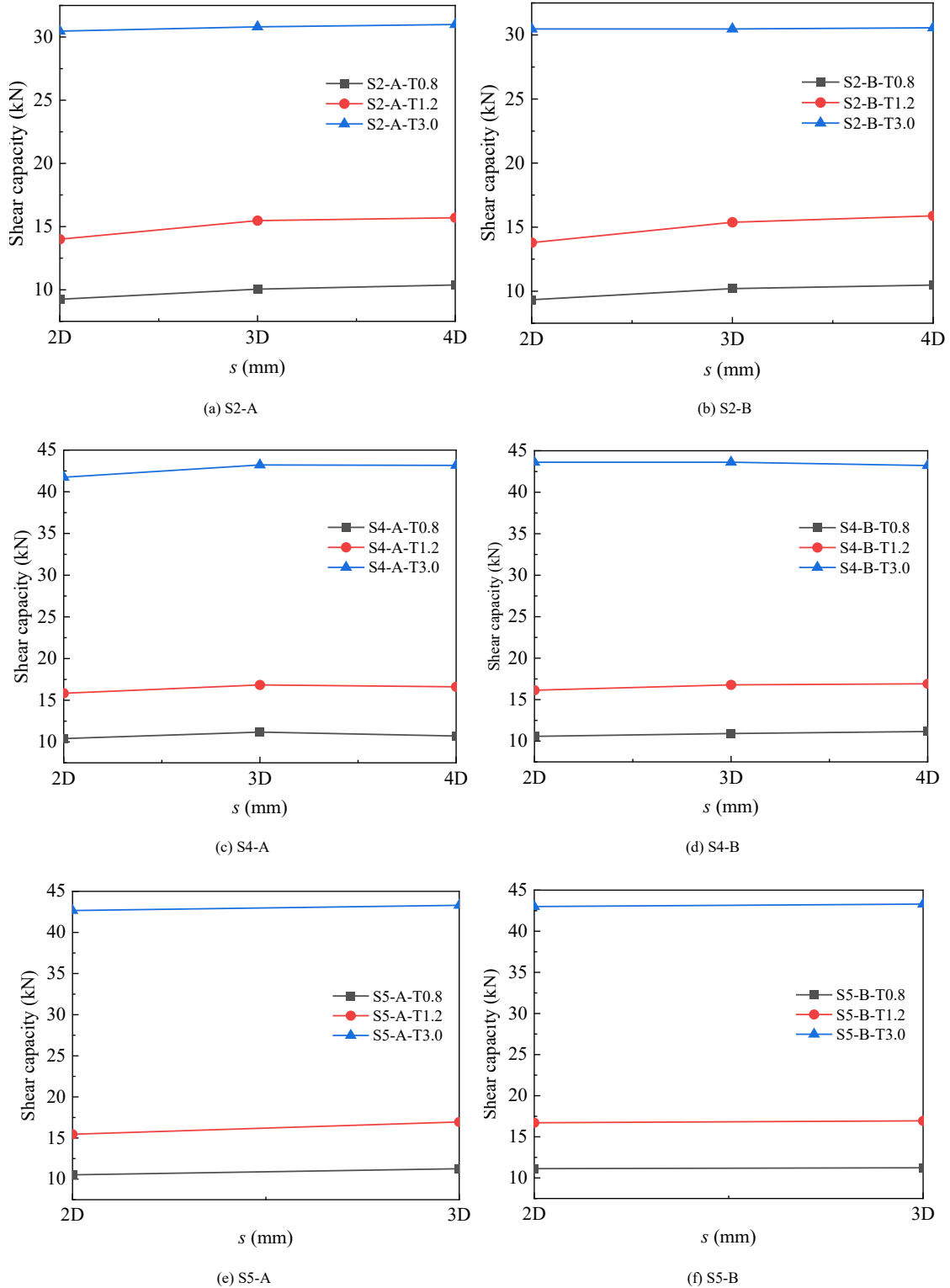


Fig. 16 Effect of  $s$  on shear capacity

4.3.3. The influence of the screw arrangement

Table 3 presents the influence of screw arrangement on the shear capacity and peak displacement of the screw group DSCs. It can be observed from the table that, when  $s$  and  $T$  are held constant, changing the screw arrangement has

negligible impact on the shear capacity but a noticeable effect on the peak displacement. When  $n$  is 2, the peak displacement in arrangement A is generally greater than in arrangement B. However, as  $n$  increases to 4 or 5, the peak displacement in arrangement B becomes greater than in arrangement A. This can

be attributed to the fact that when  $n$  is 2 and the screw arrangement is B, the displacements of the two screw holes are independent of each other, with each screw sharing half of the external load, resulting in nearly identical displacements for the screw holes. In contrast, when the screw arrangement is A, the displacements between the two screw holes are interdependent. The displacement in the screw holes near the tensile side is larger, while the

displacement in the hole away from the tensile side is suppressed. Moreover, when multiple screws are used for the connection, a shear lag effect occurs, causing the screw holes near the tensile side to experience larger shear forces and greater deformation. As a result, for  $n = 4$  or 5, the peak displacement in arrangement B generally exceeds that in arrangement A.

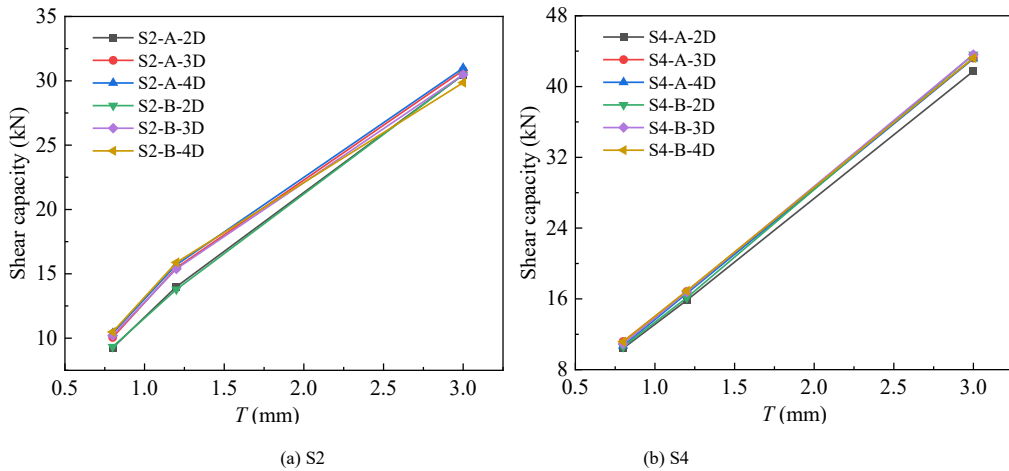
**Table 3**  
Effect of screw arrangement on shear capacity and peak displacement

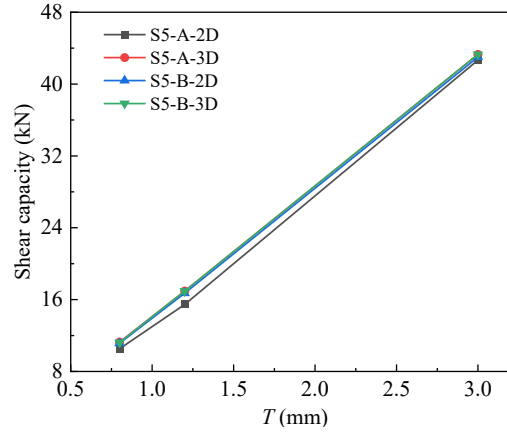
Specimen name	$P_A$ /kN	$\Delta_A$ /mm	$P_B$ /kN	$\Delta_B$ /mm	$\frac{ P_B - P_A }{P_A} \times 100\%$
S2-2D-T0.8	9.25	6.41	9.33	4.92	0.9%
S2-3D-T0.8	10.05	6.50	10.20	6.11	1.5%
S2-4D-T0.8	10.38	7.04	10.48	6.35	1.0%
S2-2D-T1.2	14.00	5.84	13.79	6.12	1.5%
S2-3D-T1.2	15.47	6.78	15.38	6.12	0.6%
S2-4D-T1.2	15.70	6.49	15.88	6.33	1.2%
S2-2D-T3.0	30.47	2.87	30.47	2.37	0.0%
S2-3D-T3.0	30.81	2.30	30.47	2.04	1.1%
S2-4D-T3.0	30.99	2.32	29.86	2.05	3.7%
S4-2D-T0.8	10.41	4.39	10.58	5.75	1.6%
S4-3D-T0.8	11.18	5.06	10.92	5.34	2.3%
S4-4D-T0.8	10.71	4.65	11.16	5.60	4.2%
S4-2D-T1.2	15.84	5.25	16.14	6.15	1.9%
S4-3D-T1.2	16.84	5.53	16.78	5.43	0.4%
S4-4D-T1.2	16.61	5.30	16.91	5.84	1.8%
S4-2D-T3.0	41.74	6.33	43.62	6.89	4.5%
S4-3D-T3.0	43.22	6.53	43.62	6.89	0.9%
S4-4D-T3.0	43.16	6.33	43.22	6.47	0.1%
S5-2D-T0.8	10.52	4.18	11.13	5.36	5.8%
S5-3D-T0.8	11.27	5.36	11.23	5.38	0.4%
S5-2D-T1.2	15.46	6.49	16.71	5.34	8.1%
S5-3D-T1.2	16.95	5.49	16.94	5.68	0.1%
S5-2D-T3.0	42.67	6.04	43.01	6.40	0.8%
S5-3D-T3.0	43.30	6.16	43.30	6.19	0.0%

4.3.4. The influence of sheet thickness

Fig. 17 displays the relationship curves between shear capacity and sheet thickness ( $T$ ). It is observed that the shear capacity increases almost linearly with  $T$ . Specifically, the shear capacity of screw group DSCs increases by at least

51.1% when  $T$  rises from 0.8 mm to 1.2 mm. When  $T$  increases from 1.2 mm to 3.0 mm, the shear capacity increases by a maximum of 176.0% and a minimum of 88.0%. These results demonstrate that the sheet thickness has a remarkable impact on the shear capacity of screw group DSCs.





(c) S5

Fig. 17 Effect of  $T$  on shear capacity

## 5. Evaluation of design formulas

### 5.1. Design formulas for single screw SSCs

Currently, design formulas for predicting the shear capacity of single screw SSCs are available in AISI S100-2016 [29], GB 50018-2002 [30], EN 1993-1-3:2006 [31], and AISC 360-16 [32]. The specific forms of these formulas are as follows.

#### 5.1.1. Screw shear failure

AISI S100-2016, GB 50018-2002, and EN 1993-1-3:2006 specify the shear capacity of single screw SSCs as shown in Eq. (1):

$$P_n = A_n F_n \quad (1)$$

where  $A_n$  indicates the screw cross-sectional area,  $F_n$  is the screw shear capacity, taken as 225MPa [28].

AISC 360-16 [32] specifies that the design shear capacity of the connections as:

$$P_n = \phi A_n F_{nv} \quad (2)$$

Where  $F_{nv} = 0.45F_u$ ,  $\phi = 0.75$ .

#### 5.1.2. Screw tilting accompanied by bearing failure

AISI S100-2016 defines the shear capacity as follows:

(1) When  $t_2/t_1 \leq 1.0$ , the shear capacity of single screw SSCs takes the minimum value of Eqs. (3)~(5).

$$P_n = 4.2\sqrt{t_2^3 d} F_{u2} \quad (3)$$

$$P_n = 2.7t_1 d F_{u1} \quad (4)$$

$$P_n = 2.7t_2 d F_{u1} \quad (5)$$

where  $d$  denotes the nominal screw diameter,  $t_1$  and  $t_2$  represent the sheet thickness in contact with and away from the screw head, respectively, and  $F_{u1}$  and  $F_{u2}$  denote the sheet strength in contact with and away from the screw head, respectively.

(2) When  $t_2/t_1 \geq 2.5$ , the shear capacity of single screw SSCs takes the minimum value of Eqs. (6)~(7).

$$P_n = 2.7t_1 d F_{u1} \quad (6)$$

$$P_n = 2.7t_2 d F_{u1} \quad (7)$$

(3) When  $1.0 < t_2/t_1 < 2.5$ , the shear capacity of single screw SSCs is a linear interpolation of the two aforementioned scenarios.

GB 50018-2002 states:

(1) When  $t_1/t = 1.0$ , the shear capacity of single screw SSCs is calculated by Eq. (8).

$$P_n = 3.7\sqrt{t^3 d} f \quad \text{and} \quad P_n \leq 2.4tdf \quad (8)$$

where  $t$  represents the thinner plate thickness, respectively,  $t_1$  denotes the thicker plate thickness;  $f$  indicates the design tensile strength of the steel plate being connected.

(2) When  $t_1/t \geq 2.5$ , the shear capacity of single screw SSCs is derived by Eq. (9).

$$P_n \leq 2.4tdf \quad (9)$$

(3) When  $1.0 < t_1/t < 2.5$ , the shear capacity of single screw SSCs is a linear interpolation of the two aforementioned scenarios.

EN 1993-1-3:2006 provides for the shear capacity for screw SSC specimens as determined by Eq. (10).

$$P_n = \alpha F_u dt \quad (10)$$

Where

$$\alpha = 3.2\sqrt{t_1/d} \leq 2.1, \quad t_2/t_1 = 1.0;$$

$$\alpha = 3.2\sqrt{t_1/d} \leq 2.1, \quad t_2/t_1 \geq 2.5, \quad t_1 < 1.0\text{mm};$$

$$\alpha = 2.1, \quad t_2/t_1 \geq 2.5, \quad t_1 \geq 1.0\text{mm};$$

When  $1.0 < t_2/t_1 < 2.5$ ,  $\alpha$  is determined by linear interpolation.

AISC 360-16 specifies that the shear capacity of single screw SSCs is calculated by Eq. (11).

$$P_n = 2.4\phi F_u dt \quad (11)$$

where  $\phi = 0.75$ ,  $F_u$  denotes the sheet strength.

### 5.2. Design formulas for screw group SSCs

The shear capacity and reduction coefficient for the screw group SSC specimens can be derived from Eq. (12) and Eq. (13), respectively.

$$P = nP_1 R_L \quad (12)$$

$$R_L = \left( 0.535 + \frac{0.467}{\sqrt{n}} \right) \leq 1.0 \quad (13)$$

where  $P_1$  stands for the shear capacity of single screw SSCs;  $P$  represents the shear capacity of screw group SSCs;  $n$  denotes the number of screws;  $R_L$  represents the group effect reduction coefficient.

### 5.3. Comparison of FE values with predicted results

#### 5.3.1. Comparison of shear capacity of single screw DSCs

Since the shear capacity formulas of the current specifications are only applicable to screw SSCs, the shear capacity of single screw DSCs can be calculated by adapting the formulas for screw SSCs and DSCs. Specifically, the

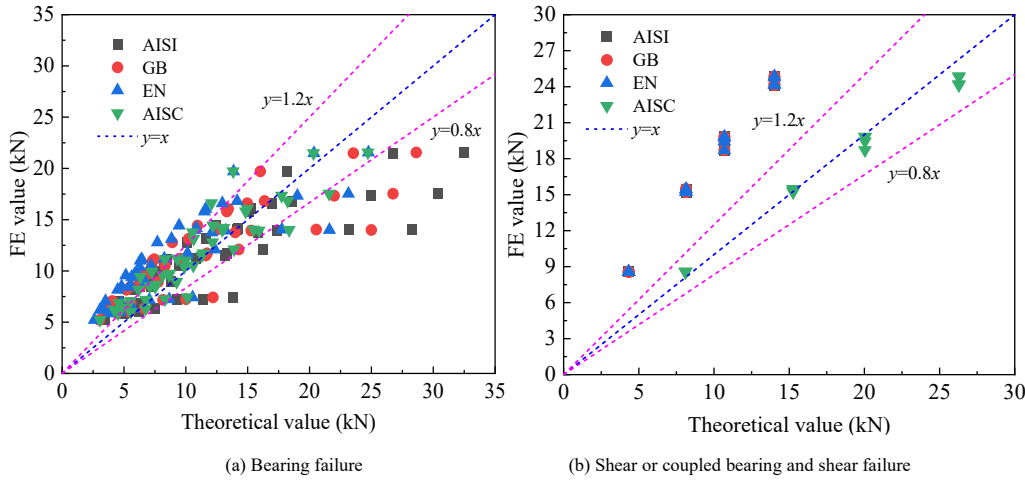
shear capacity of screw DSCs is obtained by multiplying the SSCs shear capacity formulas by a coefficient  $n_s$ , where  $n_s = 2$ , indicating the presence of two shear surfaces. In addition, it is noticed that when shear failure or coupled bearing and shear failure occurs, the difference in the shear capacity between the specimens is not significant, so the same calculation formula is applied to both failure modes.

Table 4 provides a statistical analysis of the FE and theoretical shear capacity of screw DSCs, where  $P_u$  and  $P_n$  denote the FE and theoretical values, respectively. Table 4 shows that the design formulas of the GB, EN, and AISC specifications tend to be conservative when specimens undergo bearing failure. Specifically, the shear capacity of screw DSCs is underestimated by 19%, 38%, and 13%, respectively, with the average predicted shear capacity from the AISC

specification being closest to the FE values. In addition, as shown in Fig. 18(a), when specimens experience bearing failure, the errors between the FE and theoretical values can reach up to 20%. Although the Chinese, American, and European specifications tend to be more conservative, some predicted values are biased towards being unsafe. Overall, the AISC specification provides a better agreement with the FE values. In cases of shear failure, the AISI, GB, and EN specifications are excessively conservative, with the shear capacity being underestimated by 86%. As seen in Fig. 18(b), the predicted values from the AISC specification align well with the FE values, with errors between the two being less than 20%. In conclusion, the AISC specification is more suitable for evaluating the shear capacity of single screw DSCs, regardless of whether bearing or shear failure occurs.

**Table 4**  
Statistical characteristics on  $P_u/P_n$  for single screw DSCs

Failure modes	Number of specimens		$P_u/P_n$			
			AISI	GB	EN	AISC
Bearing failure	47	Mean	1.05	1.19	1.38	1.13
		COV/%	26.4%	26.5%	26.5%	18.5%
Shear/Coupled bearing and shear failure	16	Mean	1.86	1.86	1.86	0.99
		COV%	4.8%	4.8%	4.8%	4.8%



**Fig. 18** Comparison of FE values with theoretical values for single screw DSCs

5.3.2. Comparison of shear capacity of screw group DSCs

Table 5 provides the statistical results of the FE versus predicted values of screw group DSCs. In addition, Fig. 19 shows the comparison of FE values with predicted values. Combined with Table 5 and Fig. 19, it is observed that when the specimen experiences bearing failure, the predicted shear capacity is insecure, with the average shear capacity being overestimated by 26% and the coefficient of variation reaching 27.11%. When the specimen undergoes coupled bearing and shear failure, the predicted shear capacity is more conservative, with the mean capacity underestimated by 16% and the coefficient of variation reduced to 1.16%. Therefore, the prediction equations can be employed to evaluate the shear capacity of specimens under coupled bearing and shear failure. However, for specimens undergoing bearing failure, the errors between most predicted and FE values exceed 20%, indicating that the existing prediction formulas are not suitable for assessing the shear capacity of screw group DSCs.

**Table 5**  
Statistics on the ratio of FE values to predicted values for screw group DSCs

Failure mode	Number of specimens		$P_u/P_n$	$P_u/P_c$
Bearing failure	36	Mean	0.74	1.25
		COV/%	27.11	29.62
Coupled bearing and shear failure	6	Mean	1.16	/
		COV%	1.16	/

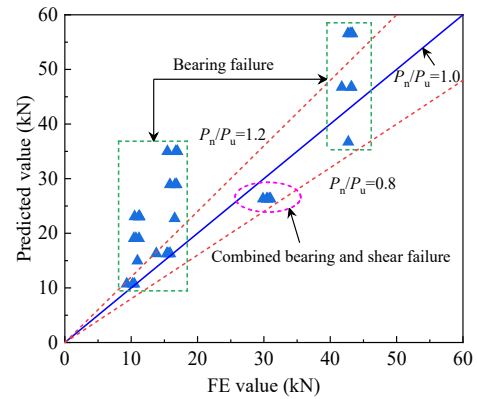


**Fig. 19** Comparison of FE values with predicted values for screw group DSCs

5.4. Design formula modification

From the analyses in subsection 5.3.3, it is found that when the specimen undergoes bearing failure, the calculated shear capacity of screw group DSCs tends to be unsafe. Therefore, the existing equations for calculating the shear capacity of screw group DSCs have been modified, as shown in Eqs. (14)-(15). The comparison between the calculated values from the modified formula and the FE values is presented in Fig. 20. It can be observed that when the specimen experiences bearing failure, the calculated values from the modified formula are conservative.

$$P_c = anP_1R_m \tag{14}$$

$$R_m = \left( 0.535 + \frac{0.467}{\sqrt{2n}} \right) \leq 1.0 \quad (15)$$

where  $P_1'$  represents the shear capacity of single screw DSCs, and  $\alpha$  indicates the shear capacity modification factor. When  $T = 3.0$  mm and  $n > 2$ , the specimen primarily experiences bearing failure, with the screw shank undergoing significant shear deformation, in which case  $\alpha = 0.9$ . For all other cases,  $\alpha = 0.6$ .  $P_c$  denotes the modified shear capacity of screw group DSCs, where  $n$  is the number of screws, and  $2n$  indicates the number of screw shear surfaces.  $R_m$  is the modified group effect reduction factor.

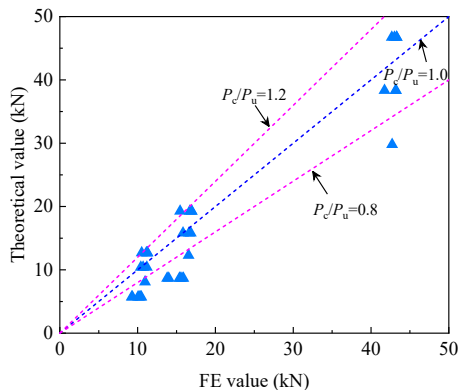


Fig. 20 Comparison of FE values and modified shear capacity of screw group DSCs

## 6. Conclusion

This study investigated the shear performance of screw DSCs using a validated FE model. The effects of steel strength, sheet thickness, screw diameter, screw connection types, number of screws, screw spacing, and screw arrangement on the failure modes and shear capacity of screw DSCs were discussed. Finally, the results of the parametric analyses were used to evaluate the applicability and feasibility of existing design formulas for predicting the shear capacity of single screw and screw group DSCs. The main conclusions are as follows:

- (1) The parametric analysis results show that the shear capacity increases with steel strength when the sheet thickness is less than 3.0 mm. The shear capacity initially increases with sheet thickness and eventually stabilizes. Additionally, the shear capacity increases almost linearly with screw diameter. Notably, the shear capacity of screw DSCs is significantly higher than that of screw SSCs, although the relationship is not a simple twofold correlation.
- (2) The failure modes of screw group DSCs can be classified into two types: bearing failure and coupled bearing and shear failure. Both the number of screws and the steel plate thickness significantly influence the failure mode of screw group DSCs. However, when the number of screws exceeds 2, further increases in the number of screws do not affect the failure mode. Screw spacing and screw arrangement have a minimal effect on the failure mode.
- (3) The shear capacity of screw group DSCs increases with the number of screws. When the sheet thickness reaches 3.0 mm and the number of screws increases to 3, the failure mode changes from coupled bearing and shear failure to bearing failure. Beyond this point, further increases in the number of screws have minimal impact on the shear capacity. The effect of screw spacing on the shear capacity diminishes as the number of screws increases. While the screw arrangement has little effect on the shear capacity, it significantly impacts the peak displacement. Additionally, the shear capacity of screw group DSCs increases almost linearly with an increase in plate thickness.
- (4) The evaluation results show that the predictions from the AISC specification formulas agree well with the FE values, regardless of whether bearing or shear failure occurs in single-screw DSCs. Therefore, the AISC specification is more suitable for evaluating the shear capacity of single-screw DSCs. In addition, the current specifications tend to be more conservative when evaluating the shear capacity of single-screw SSCs.
- (5) When evaluating the shear capacity of screw group DSCs, it is found that the predicted shear capacity is not conservative in cases of bearing failure. However, the modified shear capacity for screw group DSCs is conservative, ensuring compliance with the requirements for a biased safe design. In cases of coupled bearing and shear failure, the predicted shear

capacity remains on the conservative side.

## Declaration of competing interests

The authors declare that they have no known competing financial interests or personal relationships that could have appeared to influence the work reported in this paper.

## Acknowledgments

The authors gratefully acknowledge the financial support provided by the Science and Technology Innovation Plan Project of Hunan Province (Grant 2018NK2053) and Changsha Excellent Innovative Youth Training Program (Project No. kq1802001).

## Reference

- [1] W.H. Liu, L. Deng, W.J. Zhong, Y.L. Yang, Parametric study on the pull-out performance of screw connections in cold-formed thin-walled steel structures, *Eng. Struct.* 274 (2023): 115007, <https://doi.org/10.1016/j.engstruct.2022.115007>.
- [2] Y.H. Xing, O. Zhao, W.Y. Wang, Testing, modelling and analysis of full-scale cold-formed steel center-sheathed shear walls in fire, *Eng. Struct.* 284 (2023): 115970, <https://doi.org/10.1016/j.engstruct.2023.115970>.
- [3] T. Pekoz, Design of cold-formed steel screw connections, International Specialty Conference on Cold-formed Steel Structures, 1990.
- [4] C.A. Rogers, G.J. Hancock, Screwed connection tests of thin G550 and G300 sheet steels, *J. Struct. Eng.* 125 (2) (1999): 128-136, [https://doi.org/10.1061/\(ASCE\)0733-9445\(1999\)125:2\(128\)](https://doi.org/10.1061/(ASCE)0733-9445(1999)125:2(128)).
- [5] R.A. Laboube, M.A. Sokol, Behavior of screw connections in residential construction, *J. Struct. Eng.* 128 (1) (2002): 115-118, [https://doi.org/10.1061/\(ASCE\)0733-9445\(2002\)128:1\(115\)](https://doi.org/10.1061/(ASCE)0733-9445(2002)128:1(115)).
- [6] S. Seleim, R.A. Laboube, Behavior of low ductility steels in cold-formed steel connections, *Thin-Walled Struct.* 25 (2) (1996): 135-151, [https://doi.org/10.1016/0263-8231\(95\)00039-9](https://doi.org/10.1016/0263-8231(95)00039-9).
- [7] M.A. Sokol, R.A. Laboube, W. Yu, Determination of the tensile and shear strengths of screws and the effect of screw patterns on cold-formed steel connections, Center for Cold Formed Steel Structures Library, 1998, 1-172.
- [8] K. Roy, H.H. Lau, T.C.H. Ting, R. Masood, A. Kumar, J.B.P. Lim, Experiments and finite element modelling of screw pattern of self-drilling screw connections for high strength cold-formed steel, *Thin-Walled Struct.* 145 (2019): 106393, <https://doi.org/10.1016/j.tws.2019.106393>.
- [9] M.T. Huynh, C.H. Pham, G.J. Hancock, Experimental behaviour and modelling of screwed connections of high strength sheet steels in shear, *Thin-Walled Struct.* 146 (1) (2020): 106357, <https://doi.org/10.1016/j.tws.2019.106357>.
- [10] M.T. Huynh, C.H. Pham, G.J. Hancock, Design of screwed connections in cold-formed steels in shear, *Thin-Walled Struct.* 154 (5) (2020): 106817, <https://doi.org/10.1016/j.tws.2020.106817>.
- [11] W. Lu, M. Pentti, J. Outinen, Z.C. Ma, Design of screwed steel sheeting connection at ambient and elevated temperatures, *Thin-Walled Struct.* 49 (12) (2011): 1526-1533, <https://doi.org/10.1016/j.tws.2011.07.014>.
- [12] S.T. Vy, M. Mahendran, Screwed connections in built-up cold-formed steel members at ambient and elevated temperatures, *J. Constr. Steel Res.* 192 (2022): 107218, <https://doi.org/10.1016/j.jcsr.2022.107218>.
- [13] W. Chen, J.H. Ye, M.Y. Zhao, Steady-and transient-state response of cold-formed steel-to-steel screwed connections at elevated temperatures, *J. Constr. Steel Res.* 144 (2018): 13-20, <https://doi.org/10.1016/j.jcsr.2018.01.016>.
- [14] G. Quan, J. Ye, W.C. Li, Computational modelling of cold-formed steel lap joints with screw fasteners, *Structures* 33 (2021): 230-245, <https://doi.org/10.1016/j.istruc.2021.04.062>.
- [15] Z.H. Chen, X.Y. Niu, J.D. Liu, K. Khan, Experimental study of thin-walled steel-timber single-shear connection with a self-tapping screw, *Structures* 34 (2021): 4389-4405, <https://doi.org/10.1016/j.istruc.2021.10.028>.
- [16] R.Q. Feng, Q. Cai, Y. Ma, G.R. Yan, Shear analysis of self-drilling screw connections of CFS walls with steel sheathing, *J. Constr. Steel Res.* 167 (2020): 105842, <https://doi.org/10.1016/j.jcsr.2019.105842>.
- [17] L.F. Lu, D. Wang, W. Wang, H.H. Wu, K. Ding, K.K. Darkwah, H.W. Yan, Shear bearing capacity of self-drilling screw group connections of CFS sheets, *Structures* 35 (2021): 160-171, <https://doi.org/10.1016/j.istruc.2021.10.096>.
- [18] E. Varoglu, E. Karacabeyli, S. Stiemer, C. Ni, Midply wood shear wall system: Concept and performance in static and cyclic testing, *J. Struct. Eng.* 132 (9) (2006): 1417-1425, [https://doi.org/10.1061/\(ASCE\)0733-9445\(2006\)132:9\(1417\)](https://doi.org/10.1061/(ASCE)0733-9445(2006)132:9(1417)).
- [19] E. Varoglu, E. Karacabeyli, S. Stiemer, C. Ni, M. Buitelaar, D. Lungu, Midply wood shear wall system: performance in dynamic testing, *J. Struct. Eng.* 133 (7) (2007): 1035-1042, [https://doi.org/10.1061/\(ASCE\)0733-9445\(2007\)133:7\(1035\)](https://doi.org/10.1061/(ASCE)0733-9445(2007)133:7(1035)).
- [20] W. Zheng, W.D. Lu, W.Q. Liu, Y. Li, Lateral loading behavior of glulam frame-midply hybrid lateral systems, *Constr. Build. Mater.* 220 (2019): 53-63, <https://doi.org/10.1016/j.conbuildmat.2019.05.182>.
- [21] W. Zheng, W.D. Lu, W.Q. Liu, L. Wang, Z.B. Ling, Experimental investigation of laterally loaded double-shear-nail connections used in midply wood shear walls, *Constr. Build. Mater.* 101 (2015): 761-771, <https://doi.org/10.1016/j.conbuildmat.2015.10.100>.
- [22] X.H. Zhou, Y.X. Zou, L. Xu, X.M. Yao, Y. Shi, Y. Guan, Seismic behavior of cold-formed thin-walled steel plate shear wall, *J. Build. Struct.* 5 (2020): 65-75.
- [23] V. Briere, V. Santos, C.A. Rogers, Cold-formed steel centre-sheathed (mid-ply) shear walls, *Soil Dyn. Earthq. Eng.* 114 (11) (2018): 253-266, <https://doi.org/10.1016/j.soildyn.2018.07.008>.
- [24] R. Deng, L. Ye, Y. Gao, Y. Shi, Y.H. Wang, Behaviour of cold-formed steel framed shear walls with slitted sheathing under lateral loading, *Thin-Walled Struct.* 192 (2023): 111108, <https://doi.org/10.1016/j.tws.2023.111108>.
- [25] J.C. Wu, C.A. Rogers, Cold-formed steel centre-sheathed (mid-ply) shear walls of intermediate resistance, *Thin-Walled Struct.* 188 (2023): 110834, <https://doi.org/10.1016/j.tws.2023.110834>.
- [26] N. Yanagi, C. Yu, Effective strip method for the design of cold-formed steel framed shear wall

- with steel sheathing, *J. Struct. Eng.* 140 (4) (2013): 04013101, [https://doi.org/10.1061/\(ASCE\)ST.1943-541X.0000870](https://doi.org/10.1061/(ASCE)ST.1943-541X.0000870).
- [27] L.N. Zhou, Y.H. Chui, C. Ni, Influence of middle member thickness on properties of double-shear nail joints, *J. Struct. Eng.* 144 (8) (2018): 04018109, [https://doi.org/10.1061/\(ASCE\)ST.1943-541X.0002126](https://doi.org/10.1061/(ASCE)ST.1943-541X.0002126).
- [28] N. Liu, Research on shear behavior and design method of self-tapping screw connecting, Heilongjiang: Harbin Institute of Technology, 2007.
- [29] AISI S100-2016, North American Specification for the Design of Cold-Formed Steel Structural Members. Washington D.C.: American Iron and Steel Institute, 2016.
- [30] GB 50018-2002, Technical code of cold-formed thin-walled steel structures. Beijing: China Planning Press, 2002.
- [31] EN 1993-1-3:2006, Eurocode 3, Design of Steel Structures - Part 1-3 General Rules - Supplementary Rules for Cold-formed Members and Sheeting. Brussels: The European Committee for Standardization, 2006.
- [32] ANSI/AISC 360-16, Specification for structural steel buildings, American Institute of Steel Construction, 2016.
- [33] L.F. Lu, Y.P. Zhang, W.Q. Fang, D.H. Yang, Experimental investigation and numerical analysis on shear-bearing capacity for self-drilling screw connections of cold-formed thin-walled steel II: Numerical analysis, *J. Cent. South Univ. (Science and Technology)*. 44 (8) (2013): 3493-3502.
- [34] J. Choung, C.S. Shim, H.C. Song, Estimation of failure strain of EH36 high strength marine structural steel using average stress triaxiality, *Mar. Struct.* 29 (1) (2012): 1-21, <https://doi.org/10.1016/j.marstruc.2012.08.001>.
- [35] X.L. Zhang, Y.C. Zhang, Finite element analysis for shearing resistance of screw connections in crest-fixed profiled steel sheeting, *Progress in Steel Building Structures*. 12 (2) (2010): 23-29.
- [36] Y. Shi, X.H. Zhou, Y. Guan, X.M. Yao, Study on mechanical behavior and effective length of cold-formed thin-walled steel roof truss, *J. Build. Struct.* 40 (11) (2019): 65-75.
- [37] G. Shi, X. Zhu, Study on constitutive model of high-strength structural steel under monotonic loading, *Eng. Mech.* 34 (2) (2017): 50-59.